Then in the stationary state the number of particles being scattered into (μ) in time dt can be written in two ways:

$$N_0P(\mu)dt=\sum P(\nu)Q(\mu|\nu)N_0dt,$$

i.e.,

$$P(\mu)=\sum_\nu P(\nu)Q(\mu|\nu).$$

For isotropic scattering, instead of the momentum-space cells, energy cells dE can be introduced. This leads to Eq. (3).

PHYSICAL REVIEW VOLUME 184, NUMBER 3 15 AUGUST 1969

Analysis of the Tunneling Measurement of Electronic Self-Energies Due to Interactions of Electrons and Holes with Optical Phonons in Semiconductors*

L. C. Davis† and C. B. Duke
Department of Physics and Materials Research Laboratory, University of Illinois, Urbana, Illinois 61801
(Received 27 February 1969)

The electronic self-energies in degenerate semiconductors due to interactions of electrons and holes with optical and local-mode phonons (of energy $\hbar\omega_0$) are evaluated using second-order perturbation theory. Both (screened) polar and deformation-potential interactions are considered, as are the effects of optical-phonon dispersion: $\hbar\omega(\mathbf{q})=\hbar\omega_0-\alpha q^2$. One-electron models of tunneling in metal-oxide-semiconductor junctions are constructed. Their consequences are investigated numerically for indium-SiO_2-silicon junctions. The results of these calculations are parametrized by simple models of the barrier penetration factor for use in evaluating fine structure at $eV\cong\pm\hbar\omega_0$ due to electron-phonon interactions. The transfer-Hamiltonian model is utilized to classify such fine structure as due to either inelastic tunneling processes or (electrode) self-energy effects. The analytical and experimental distinction between these two types of effects is described. The combined model obtained using second-order self-energies characteristic of the semiconductor electrode and simplified approximate barrier penetration factors is utilized to interpret experimental data on indium-SiO_2-silicon and Au-CdS junctions. The satisfactory description of these data suggests that d^2I/dV^2 measurements on junctions in which one electrode is a very heavily doped semiconductor can provide a direct experimental determination of the energy-shell electronic self-energies in the semiconductor electrode.

I. INTRODUCTION

THE first clear observation via electron tunneling of the influence of electronic interactions with other elementary excitations characteristic of a tunnel junction was the identification in 1959 of phonon-assisted tunneling in p-n tunnel diodes.[1–3] In order to relate this "inelastic tunneling" process to the "self-energy" effects considered in this paper, it is convenient (but not necessary) to utilize the transfer-Hamiltonian model.[3–6] Within the framework of this model, a tunnel junction is regarded as two electrodes, described by $\mathcal{H}_L$ and $\mathcal{H}_R$, respectively, weakly coupled by a transfer Hamiltonian T which transfers electrons from one electrode to the other. The total Hamiltonian is given by

$$\mathcal{H}=\mathcal{H}_L+\mathcal{H}_R+T. \tag{1.1}$$

The tunneling current I is evaluated[3,5,6] via obtaining the linear response of the isolated electrodes, described by $\mathcal{H}_0=(\mathcal{H}_L+\mathcal{H}_R)$, to T.

An inelastic tunneling process is defined to be one described by a term in the transfer Hamiltonian of the form[3,6]

$$T_{\text{in}}=\sum_{\mathbf{k},\mathbf{q},\mathbf{p}}[\Lambda_{\mathbf{k},\mathbf{q}}(\mathbf{p})c_{\mathbf{k}}{}^\dagger c_{\mathbf{q}}(a_{\mathbf{p}}{}^\dagger+a_{\mathbf{p}})+\text{H.c.}]. \tag{1.2}$$

The $c_{\mathbf{k}}$ are the annihilation operators of electrons in the right-hand electrode, the $c_{\mathbf{q}}$ are those of electrons in the left-hand electrode, and the $a_{\mathbf{p}}$ ($a_{\mathbf{p}}{}^\dagger$) are the annihilation (creation) operators of the (boson) elementary excitation created during the inelastic tunneling process. In terms of a diagrammatic description of tunneling,[3,6] inelastic channels are described by diagrams like that shown in Fig. 1 in which solid lines denote electron propagators in the electrodes and wavy lines denote boson propagators describing excitations [e.g., phonons] created by a tunneling electron. If the tunneling electrons create excitations in a narrow energy region $E\cong\hbar\omega_0$, then for values of the bias V across the tunnel junction such that $|eV|\cong\hbar\omega_0$, the conductance

* Work was supported in part by the Advanced Research Projects Agency under Contract No. SD-131.
† National Science Foundation postdoctoral fellow. Present address: Ford Scientific Labs., Dearborn, Michigan 48121.
[1] N. Holonyak, Jr., I. A. Lesk, R. N. Hall, J. J. Tiemann, and H. Ehrenreich, Phys. Rev. Letters 3, 167 (1959).
[2] L. Esaki and Y. Miyahara, Solid State Electron. 1, 13 (1960).
[3] C. B. Duke, *Tunneling in Solids* (Academic Press Inc., New York, 1969), Chaps. 6, 7.
[4] J. Bardeen, Phys. Rev. Letters 6, 57 (1961).
[5] M. H. Cohen, L. M. Falicov, and J. C. Phillips, Phys. Rev. Letters 8, 316 (1962).
[6] A. J. Bennett, C. B. Duke, and S. D. Silverstein, Phys. Rev. 176, 969 (1968).

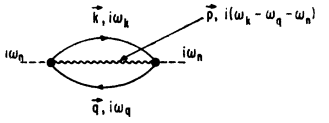

FIG. 1. Diagrammatic description of the contribution to the tunneling current due to a single-boson-emission inelastic process. A detailed description of the evaluation of the contribution to the current denoted by this diagram is given in Sec. 19 of Ref. 3 and in Ref. 6.

dI/dV exhibits sharp increases.[1–3,6,7] If the electrons are coupled to a wide band of excitations $E \leq \hbar\omega_0$, approximately symmetric conductance minima occur at zero bias.[6,8] The outstanding characteristic of inelastic tunneling predicted by the transfer-Hamiltonian model is the threshold nature of such processes resulting in approximately symmetric increases in the conductance for both polarities of the bias voltage.

This paper is devoted to an investigation of the consequences of electron-phonon interactions in the electrode Hamiltonians $\mathcal{H}_L$ and $\mathcal{H}_R$ rather than in the transfer Hamiltonian T. For simplicity, we consider electron-phonon interactions to occur in only one of the electrodes [$\mathcal{H}_R$] and treat the transfer Hamiltonian in the (customary) elastic limit[3,4]

$$T=\sum_{\mathbf{k},\mathbf{q}} [\Lambda_{\mathbf{k},\mathbf{q}} c_{\mathbf{k}}^{\dagger} c_{\mathbf{q}} + \text{H.c.}]. \tag{1.3}$$

We refer to the consequences of the electron-phonon interactions in this limit as "self-energy" effects. They result in the transfer-Hamiltonian model from interactions in the "bulk" electrode. The diagrammatic representation of these processes (as described in this paper) is shown in Fig. 2. The consideration of electron-phonon interactions only in a single electrode provides a reasonable description of metal-semiconductor and metal-insulator-semiconductor junctions because the effects of electron-phonon interactions in the semiconductor often are considerably larger than those of the interactions in the metal (or insulator).

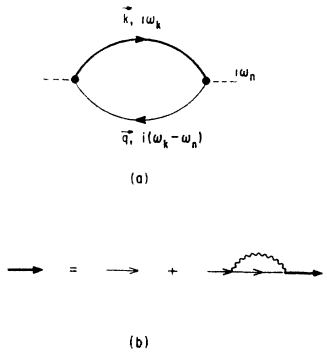

FIG. 2. (a) Diagrammatic description of the contribution to the tunneling current due to elastic transfer processes including the presence of electron self-energy corrections in the right-hand electrode. A detailed description of the evaluation of the contribution to the current denoted by this diagram is given in Secs. 19 and 20 of Ref. 3 and (in less detail) in Ref. 6. (b) Dyson equation illustrating the description of electron-phonon self-energy effects utilized in this paper. A more detailed account of this description is given in Sec. 20 of Ref. 3.

Let us assume that the left-hand electrode is a metal and the right-hand electrode is an n-type semiconductor. (The results can easily be generalized to the case where the right-hand electrode is a p-type semiconductor.) For simplicity the electrons on the left are taken to be noninteracting so that

$$\mathcal{H}_L=\sum_{\mathbf{q}} \xi_{\mathbf{q}} c_{\mathbf{q}}^{\dagger} c_{\mathbf{q}}, \tag{1.4}$$

where $\xi_{\mathbf{q}}$ is the energy of the $\mathbf{q}$th state measured relative to the metal Fermi energy. For the right-hand electrode, we utilize the model Hamiltonian

$$\mathcal{H}_R=\sum_{\mathbf{k}} \xi_{\mathbf{k}} c_{\mathbf{k}}^{\dagger} c_{\mathbf{k}} + \hbar\omega_0 \sum_{\mathbf{p}} (b_{\mathbf{p}}^{\dagger} b_{\mathbf{p}} + \tfrac{1}{2}) + \sum_{\mathbf{k},\mathbf{p}} [V_{\mathbf{p}} b_{\mathbf{p}} c_{\mathbf{k}+\mathbf{p}}^{\dagger} c_{\mathbf{k}} + \text{H.c.}], \tag{1.5}$$

where

$$\xi_{\mathbf{k}}=\hbar^2 k^2/2m^* - \zeta, \tag{1.6a}$$

$$\zeta=\hbar^2 k_F^2/2m^*, \tag{1.6b}$$

$$k_F=(3\pi^2 n)^{1/2}. \tag{1.6c}$$

The density of mobile carriers is n and the effective mass in the semiconductor electrode is m^*. The $b_{\mathbf{p}}$ are phonon annihilation operators for the semiconductor optical phonons of energy $\hbar\omega_0$. The electron-phonon interaction in the electrode is described using the Fröhlich Hamiltonian.[9]

If we apply linear-response theory,[3,10] we find that the tunneling current I is given by

$$I=\frac{4\pi e}{\hbar} \sum_{\mathbf{k},\mathbf{q}} |\Lambda_{\mathbf{k},\mathbf{q}}|^2 \int_{-\infty}^{+\infty} d\epsilon [f(\epsilon) - f(\epsilon + eV)] \delta(\epsilon - \xi_{\mathbf{q}} + eV) \times \frac{1}{\pi} \text{Im} G^R(\xi_{\mathbf{k}}, \epsilon), \tag{1.7}$$

in which ϵ denotes the total energy measured relative to the Fermi level in the semiconductor, $f(\epsilon)$ the Fermi function at $T=0°\text{K}$, V the bias voltage applied to the metal, and $G^R(\xi_{\mathbf{k}},\epsilon)$ the retarded single-particle Green's function[3] in the semiconductor electrode.

The general characteristics of self-energy effects may be exhibited by considering the expression for the tunnel conductance obtained using a simplified model in which the barrier-penetration probability [i.e., $\Lambda_{\mathbf{k},\mathbf{q}}$ in Eqs. (1.3) and (1.7)] does not depend explicitly on the bias voltage V. We find that in this case the tunnel

[7] J. Lambe and R. C. Jaklevic, Phys. Rev. **165**, 821 (1968).
[8] C. B. Duke, S. D. Silverstein, and A. J. Bennett, Phys. Rev. Letters **19**, 312 (1967).
[9] H. Fröhlich, Advan. Phys. **3**, 325 (1954).
[10] A. A. Abrikosov, L. P. Gorkov, and I. E. Dzyaloshinsky, *Methods of Quantum Field Theory in Statistical Physics* (Prentice-Hall, Inc., Englewood Cliffs, N. J., 1963), Chaps. 2–4.

conductance is given by[3,11]

$$\frac{dI}{dV}(V, T=0)=\frac{2e^2A}{\pi h}\int_{-\zeta}^{\infty} d\xi_k \, \mathrm{Im}G^R(\xi_k, -eV) \times \int \frac{d^2k_{11}}{(2\pi)^2} D(\mathbf{k}_{11},\xi_k,0). \quad (1.8)$$

The boundary condition of specular reflection has been used so we have taken[3]

$$|\Lambda_{k,q}|^2 \equiv \delta_{k_{11},q_{11}} D(\mathbf{k}_{11},\xi_k,\xi_q)/(2\pi)^2. \quad (1.9)$$

[Equation (1.9) is valid for bias functions normalized by δ functions in energy.[3]] A is the area of the planar junction.

The results of the noninteracting-electron model are readily obtained from Eq. (1.8) by taking

$$\mathrm{Im}G^R(\xi_k, -eV)=\pi\delta(\xi_k+eV), \quad (1.10a)$$

$$\frac{dI}{dV}=\frac{2e^2A}{h}\rho_{11}\int_0^{\zeta-eV} D(E_{11}, -eV, 0)dE_{11}, \quad (1.10b)$$

$$\rho_{11}=m^*/2\pi\hbar^2. \quad (1.10c)$$

Use of the approximation that D is a constant gives the linear threshold rise in the (single-particle) conductance for $eV<\zeta$ characteristic of specular tunneling into a single band as described by the WKBJ approximation.[12–14] This result is indicated schematically in Fig. 3(c) by the dashed line for the junction whose potential-energy versus distance diagram is shown in Fig. 3(a).

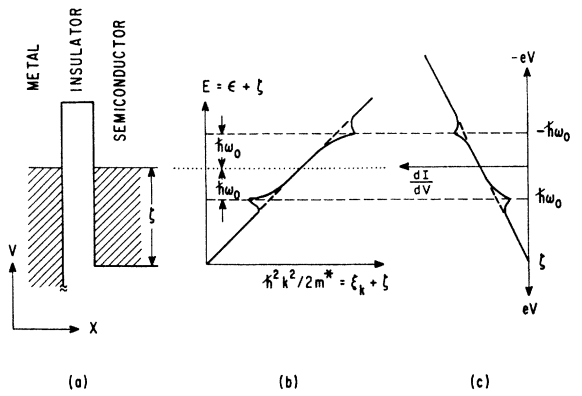

FIG. 3. (a) Schematic potential energy versus distance diagram for a metal-insulator-semiconductor junction. Energies are measured from the bottom of the semiconductor band. (b) Dispersion relation for electrons in the (degenerate) semiconductor electrode interacting with optical phonons of energy $\hbar\omega_0$. The heavy dahsed line indicates the dispersion relation in the absence of electron-phonon interactions. (c) The conductance of the metal-insulator-semiconductor tunnel junction shown in Fig. 3(a) evaluated using the constant-barrier-penetration factor model [see Eqs. (1.10) in the text and Ref. 14]. The dashed line shows the conductance predicted by this model in the absence of electron-phonon interactions in the (bulk) semiconductor electrode.

The influence of electron-phonon interactions in the electrode may be illustrated conveniently by use of the quasiparticle approximation[3] in which

$$\mathrm{Im}G^R(\xi_k,\epsilon)=Z(\epsilon)\pi\delta[\xi_k-\xi(\epsilon)]. \quad (1.11)$$

Using perturbation theory, if $\Sigma^R(\mathbf{k},\epsilon)=\Sigma(\xi_k,\epsilon)$ is the retarded[3] electronic self-energy, then $\xi(\epsilon)$ is defined to be the solution of the equation

$$\epsilon-\xi(\epsilon)-\mathrm{Re}\Sigma(\xi(\epsilon),\epsilon)=0. \quad (1.12a)$$

The quasiparticle renormalization factor $Z(\epsilon)$ is given by

$$Z(\epsilon)=(1+\partial\Sigma/\partial\xi_k)^{-1}_{\xi_k=\xi(\epsilon)}. \quad (1.12b)$$

If $Z(\epsilon)=1$, a result which occurs if $\Sigma(\mathbf{k},\epsilon)$ is a function of ϵ alone, then the entire effect of electron-phonon interactions is due to the fact that $\xi(\epsilon)\neq\epsilon$ in Eq. (1.12a). The energy-momentum relation for the electrons interacting via a deformation-potential interaction with optical phonons is shown[11] in Fig. 3(b). It is evident from Figs. 3(b) and 3(c) that even if D is constant, the phase-space restrictions due to the $\mathbf{k}_{11}$ integral in Eq. (1.8) cause a reduction in the conductance for hole injection into the semiconductor ($eV=\hbar\omega_0$) and enhancement of the conductance for electron injection ($eV=-\hbar\omega_0$). Therefore, if Σ is a function of ϵ alone, then the self-energy effects in the transfer-Hamiltonian model occur as structure at $eV\cong\pm\hbar\omega_0$ which is approximately *antisymmetric* about zero bias as shown in Fig. 3(c). Inelastic tunneling with optical-phonon emission would cause approximately *symmetrical* increases in the conductance at $eV=\pm\hbar\omega_0$. As noted in a preliminary report of this work,[11] such antisymmetric structure has been observed in tunneling characteristics of indium contacts on air-cleaved p-type silicon.[15] It subsequently has been reported due to hole-TO phonon interactions in p-type GaAs.[16]

The first interpretation of antisymmetric structure in the tunnel conductance (near the LO phonon energy) in terms of self-energy effects (in the barrier region of the semiconductor) was given by Conley and Mahan[17] for dV/dI measurements performed using gold contacts on n-type GaAs. More recent measurements[18] for indium contacts on n-type GaAs reveal a more complicated structure in d^2I/dV^2 near the LO phonon energy than the simple symmetric dispersion curves characteristic of p-type silicon[15] and GaAs.[16] This phenomenon may be due to the confluence at $\mathbf{k}\sim0$ of the TO and LO phonon energies[19,20] when $\xi\gtrsim\hbar\omega_{LO}<\hbar\omega_p=\hbar(4\pi ne^2/m^*\epsilon_\infty)^{1/2}$.

[11] L. C. Davis and C. B. Duke, Solid State Commun. **6**, 193 (1968).
[12] J. Frenkel, Phys. Rev. **36**, 1604 (1930).
[13] W. A. Harrison, Phys. Rev. **123**, 85 (1961).
[14] D. J. BenDaniel and C. B. Duke, Phys. Rev. **152**, 683 (1966); **160**, 679 (1967).
[15] E. L. Wolf, Phys. Rev. Letters **20**, 204 (1968).
[16] D. C. Tsui, Phys. Rev. Letters **21**, 994 (1968).
[17] J. W. Conley and G. D. Mahan, Phys. Rev. **161**, 681 (1967).
[18] C. B. Duke, M. J. Rice, and F. Steinrisser, Phys. Rev. **181**, 733 (1969).
[19] R. A. Cowley and G. Dolling, Phys. Rev. Letters **14**, 549 (1965).
[20] G. D. Mahan and C. B. Duke, Phys. Rev. **149**, 705 (1966).

However, the interpretation of self-energy effects due to polar coupling of holes (electrons) to LO phonons[20] also is complicated by the fact that the electronic self-energy depends on $\mathbf{k}$ as well as ϵ, so that $Z(\epsilon)$ exhibits a minimum at $\epsilon=\hbar\omega_0$ and a minimum or more complex structure at $\epsilon=-\hbar\omega_0$ (if $\hbar\omega_0<\zeta$). Although some of the experimental data suggest that this renormalization effect may not be large in very heavily doped n-type GaAs,[17] a complete analysis of the electronic self-energy due to dynamically screened polar coupling has not been given. In this paper, we follow the static screening model of Refs. 17 and 20.

It is important to recognize that the qualitative distinction between inelastic tunneling and self-energy effects based on the symmetry of the structure in dI/dV about zero bias is a distinction which is predicted only by models in which the $\mathbf{k}$ dependence of $\Sigma(\mathbf{k},\epsilon)$ is either weak or absent. Such a weak $\mathbf{k}$ dependence of the electronic self-energy is characteristic of nonpolar or heavily screened polar electron-phonon interactions. However, it is not characteristic of electron-electron interactions. For example, in the case of electron-plasmon interactions[18] the renormalization factor $Z(\epsilon)$ causes the peak at $eV=-\hbar\omega_0$ in Fig. 3(c) to be replaced by a dip. Therefore, in this case the self-energy effects cause fine structure with the same symmetry about zero bias as the inelastic-tunneling processes. As the detailed differences in line shape associated with the two phenomena are difficult to determine unambiguously from the experimental data, considerable caution must be exercised in interpreting in terms of polar electron-phonon coupling line shapes obtained using semiconductor electrodes for which $\zeta\lesssim\hbar\omega_{\mathrm{LO}}$ (so that dynamic screening occurs for some contributions to the self-energy for electron-phonon momtum transfers $|\mathbf{q}|\gtrsim k_F$).

It also is important to observe that none of the above arguments involve the dependence of $D(\mathbf{k}_{\parallel},\xi_{\mathbf{k}},\xi_{\mathbf{q}})$ on either $\mathbf{k}_{\parallel}$, $\xi_{\mathbf{k}}$, or $\xi_{\mathbf{q}}$. This result constitutes another one of the distinctions between our analysis and both the Conley-Mahan model of metal-semiconductor contacts[17] and models of self-energy effects in metallic electrodes.[21,22] These latter model calculations rely solely on the $\xi_{\mathbf{k}}$ (and $\xi_{\mathbf{q}}$) dependence of the barrier penetration probablity in order to obtain a nonzero self-energy effect. In Sec. II, we examine the sensitivity of the model predictions to the form used for the barrier penetration factor. However, in metal-insulator-semiconductor junctions, the constant-D model is often an adequate approximation to the more realistic one-electron calculations of D including space-charge effects.[14] In such junctions, the failure of particle-hole symmetry, caused by phase-space restrictions on the $\mathbf{k}_{\parallel}$ integral in Eq. (1.8), provides both the necessary and sufficient condition for the prediction of a conductance characteristic of the form shown in Fig. 3(c) if the model self-energies depend only weakly on the electron momentum variable $\mathbf{k}$.

In order to keep the presentation as simple as possible, we have arranged the paper in three main sections followed by three appendices. Section II consists of a quantitative evaluation of the tunneling line shape using the simplest reasonable model of a metal-semiconductor contact: the uniform-field model of the barrier and deformation-potential coupling of electrons to optical phonons. The detailed application of a model to the experimental situations of metal-oxide-silicon and metal-CdS junctions is also described in Sec. II. Section III contains a summary of our results and a critique of our models and of the utility of tunneling measurements as a direct experimental measurement of the phonon-induced fine structure in electronic self-energies. Those additional details whose presentation is required in order to permit independent reproduction of our calculations are given in three appendices. In Appendix A, we describe our model calculations for the electronic self-energy which are obtained by using second-order perturbation theory. Both deformation-potential and statically screened polar coupling of the electrons to optical phonons are considered together with a model for electronic interactions with local-mode phonons associated with a light (charged) impurity ion in a degenerate semiconductor.

A description of the transfer-Hamiltonian formalism and some of the difficulties associated with it is given in Appendix B. In Appendix C, the consequences of a numerical calculation of the one-electron conductance of a metal-insulator-semiconductor junction are discussed. A reasonably accurate, simple form of the barrier penetration factor is proposed and compared with the numerical calculations.

II. EVALUATION OF SIMPLE MODELS AND COMPARISON TO EXPERIMENT

The simplest reasonable model of a metal-semiconductor contact is the uniform-field model[3] of the barrier defined by

$$D=D_0\exp\left(-\frac{\hbar^2k_{\parallel}^2}{2m^*E_0}\right). \tag{2.1}$$

D_0 and E_0 are constants which can be determined by fitting the background or one-electron conductance. The uniform-field model is useful because it avoids the difficulties associated with the off-diagonal elements of $\Lambda_{\mathbf{k}\,\mathbf{q}}$ as discussed in Appendix B. Since D does not depend upon the bias V, Eq. (1.8) for the conductance is exact. Performing the $\mathbf{k}_{\parallel}$ integration in Eq. (1.8), we find

$$\frac{dI}{dV}=\frac{2e^2A}{\pi h}\rho_{\parallel}D_0E_0\int_{-\zeta}^{\infty}d\xi_{\mathbf{k}}\,\mathrm{Im}G(\xi_{\mathbf{k}},-eV)\times\{1-\exp[-(\xi_{\mathbf{k}}+\zeta)/E_0]\}, \tag{2.2}$$

[21] H. Herman and A. Schmid, Z. Physik **211**, 313 (1968).
[22] J. M. Rowell, W. L. McMillan, and W. L. Feldmann, Phys. Rev. **180**, 658 (1969).

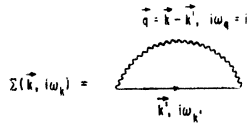

FIG. 4. Diagrammatic representation of the second-order electronic self-energy due to single-phonon emission.

where

$$\rho_{11}=m^*/2\pi\hbar^2. \tag{1.10c}$$

In addition to being useful for avoiding the difficulties of Appendix B, the uniform-field model contains the essential physical ideas which can explain the various self-energy effects observed in metal-semiconductor and metal-insulator-semiconductor contacts. To understand these self-energy effects, let us consider the effects on the tunneling conductance of the deformation-potential coupling of electrons to optical phonons. We used the expressions (A2.3) and did the integral in Eq. (2.2) numerically on the IBM 360 at the University of Illinois. The self-energy is calculated using second-order perturbation theory as shown in Fig. 4. The effects of the finite lifetime of the electrons (holes) due to their interaction with impurities and acoustical phonons[23] have been accounted for by the use of an additional phenomenological width parameter Γ_a [Eqs. (A2.5), (A2.6)].

In Fig. 5, we show the results of a numerical calculation of d^2I/dV^2 versus V for both weak and strong electron-phonon coupling. The strength of the interaction or coupling is characterized by

$$\Gamma_0(\hbar\omega_0)=\pi K^2\rho(\zeta), \tag{2.3}$$

which is the value of $|\mathrm{Im}\Sigma(\epsilon)|$ at $\epsilon=\pm\hbar\omega_0$. $\rho(\zeta)$ is the semiconductor density of states at the Fermi energy. The intrinsic width of the dispersion structure in d^2I/dV^2 is characterized by Γ_a. Its peak-to-peak height for a given Γ_a is approximately proportional to $\Gamma_0(\hbar\omega_0)$, while the separation of the peaks in voltage is given approximately by $2\Gamma_a/e$. In the weak coupling limit, the d^2I/dV^2 curve is nearly symmetric about zero bias. This is due to the fact that the $\mathrm{Re}\Sigma(\epsilon)$ is approximately an odd function of ϵ and that $\mathrm{Im}\Sigma(\epsilon)$ is small. We have shown numerically that in the weak coupling limit the pole approximation for deformation-potential coupling,

$$-\frac{1}{\pi}\mathrm{Im}G(\xi_k,\epsilon)=\delta[\xi_k-\epsilon+\mathrm{Re}\Sigma(\epsilon)], \tag{2.4}$$

gives a curve of d^2I/dV^2 versus V virtually indistinguishable from that shown in Fig. 5. The bias voltage corresponding to the center, or steepest, portion of the dispersive line shape in forward (reverse) bias is equal to $(\hbar\omega_0/e)$ $(-\hbar\omega_0/e)$.

In the strong coupling limit, the structure is not only larger than that of the weak coupling limit, but also there are differences between forward and reverse bias. This is because the imaginary part of the self-energy is important in this strong coupling limit. Large lifetime effects occur for $|\epsilon|>\hbar\omega_0$ because an electron of energy ϵ has an appreciable spectral weight in regions of higher ξ_k. Since the tunneling probability is larger for higher ξ_k, the effect of the spectral weight in regions of higher ξ_k is to open up more probable tunneling channels. This gives a behavior similar to a threshold effect at $\hbar\omega_0$ which would give a peak near $eV=\hbar\omega_0$ and a dip near $eV=-\hbar\omega_0$ in d^2I/dV^2. The lifetime effects occur in addition to the symmetric structure due to the real part of the self-energy.

Although the center of the reverse bias structure is given approximately by $-\hbar\omega_0/e$ in the strong coupling case, the peak in the forward bias structure occurs at a bias only slightly greater than $\hbar\omega_0/e$.

In both the weak and the strong coupling limits, the structure in d^2I/dV^2 is approximately the same magnitude in forward bias as it is in reverse bias. This is a consequence of the fact that structure in the self-energy is of nearly the same magnitude above and below the Fermi energy in a second-order perturbation calculation.

Measurements of the effects of the deformation-potential coupling of holes to optical phonons on the tunneling current are most extensive in p-Si.[15,24] Such measurements have also been made for p-Ge,[25] but similar effects have not been reported for n-Ge because the

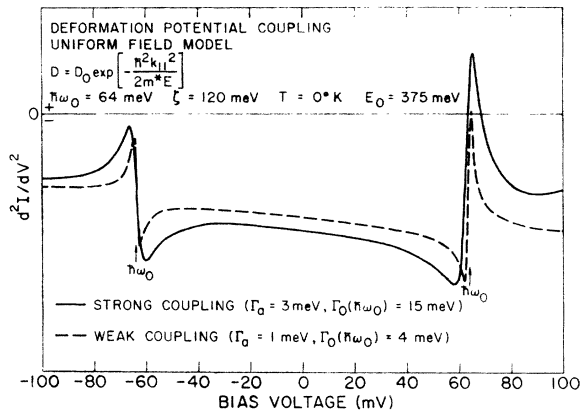

FIG. 5. Calculated d^2I/dV^2 versus V for deformation-potential coupling of electrons to optical phonons of energy $\hbar\omega_0$ (Appendix A 2) for the uniform-field model of the barrier. $\Gamma_0(\hbar\omega_0)$ characterizes the strength of the coupling. Γ_a is a phenomenological parameter characterizing the width of the structure (voltage separation of peak and dip $\simeq 2\Gamma_a/e$) due to acoustic phonon and impurity scattering. Both weak and strong coupling are shown. The vertical scale is arbitrary. The expression for the self-energy used in these calculations is given by Eqs. (A2.2)–(A2.6) and the barrier-penetration factor is given by Eq. (2.1).

[23] E. M. Conwell, *High Field Transport in Semiconductors*, (Academic Press Inc., New York, 1967), Chap. 6.

[24] W. D. Compton and D. Cullen (private communication).

[25] F. Steinrisser, L. C. Davis, and C. B. Duke, Phys. Rev. **176**, 912 (1968).

coupling is an order of magnitude weaker.[23] Due to the symmetry of the conduction-band wave functions in n-Si, the matrix element describing the interaction of electrons with optical phonons in this material is of a different form.[23,26] It has also been suggested that the observation of the TO phonon in p-GaAs tunnel junctions is due to deformation potential coupling.[16]

In Fig. 6, a comparison of a model calculation to the experimental data (d^2I/dV^2 versus V) for an In-SiO_2-Si system[24] is shown. The calculation was done for a barrier penetration factor of the form

$$D=D_0\exp\left[\frac{eV}{E_1}+\frac{\xi_q}{E_0}-\frac{\hbar^2k_{11}^2}{2m^*E_0}\right]. \tag{2.5}$$

Equation (2.5) is appropriate for a metal-insulator-semiconductor junction where the tunneling is via a conduction band in the insulator and the semiconductor is p type (see Appendix C). For simplicity, we take the effective mass in the insulator to be the same as the hole mass m^* in the semiconductor. Corrections to the conductance of the form specified by Eq. (C11) were included in the calculation to account for the bias dependence of D. These corrections are, in general, rather small and give only minor modifications of the line shapes. The form of $\Sigma(\epsilon)$ was taken to be that given by Eq. (A2.3) with an additional width parameter Γ_a (as in Fig. 5).

The values of $\Gamma_0(\hbar\omega_0)$ and Γ_a were chosen to give a reasonable fit to the experimental line shapes. The value of $\hbar\omega_0$ in this calculation was taken to be 64 meV which is less than the measured value for $k=0$ phonons in Si, 64.9 meV.[27] This smaller value of $\hbar\omega_0$ was chosen to account for the effects of phonon dispersion on $\Sigma(\epsilon)$. Dispersion tends to shift the structure in $\Sigma(\epsilon)$ to lower values of $|\epsilon|$. Other parameters were chosen to agree with the one-electron or background conductance.

It can be seen in Fig. 6 that the qualitative features of the model are in good agreement with experiment. In particular, the structure in d^2I/dV^2 is of the proper symmetry, namely, symmetric with respect to zero bias. The outstanding feature of these self-energy effects, the symmetric line shape in d^2I/dV^2, is clearly distinguishable from the antisymmetric line shape expected in d^2I/dV^2 when inelastic phonon emission occurs. The correctness of the symmetry predicted by our calculation constitutes the strongest evidence for the validity of the self-energy mechanism. We reemphasize that this prediction does *not* depend on the model used for the barrier penetration factor.

Although the shape of the calculated reverse bias structure closely resembles the experimental curve, the size of the calculated structure appears to be too large. There are, however, important corrections to the experimental line shapes due to the fact that the conductance dI/dV is rapidly increasing in reverse bias.[28] The corrections are much smaller in forward bias where the conductance is lower. A comparison of the calculated line shape to the corrected experimental line shape is shown in Fig. 7. The apparent discrepancy in the size of the reverse bias structure in Fig. 6 is much less when these experimental corrections are considered (Fig. 7).

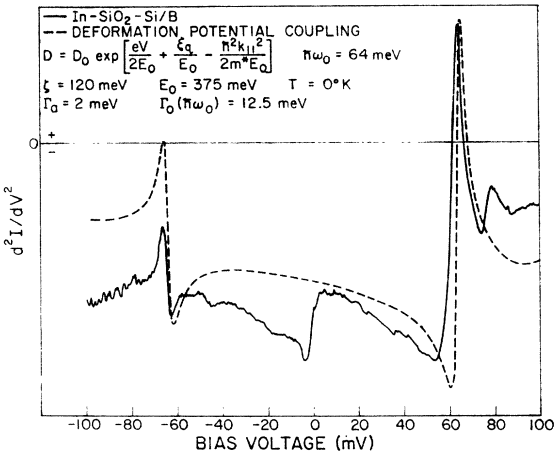

FIG. 6. The model calculation for deformation-potential coupling of optical phonons to holes in p-Si (dashed curve) is compared to the experimental data (solid curve) for In-$SiIO_2$-Si junction see Ref. 24). Si electrode doped with $\sim10^{20}$ B impurities. No corrections to experimental curve due to low-junction resistance in reverse bias have been made (see Ref. 28). The vertical scale is arbitrary. The expression for the self-energy used in the model calculation is given by Eqs. (A2.2)–(A2.6) and the barrier-penetration factor is given by Eq. (C9b) with $E_1=2E_0$. The model calculation also includes the contribution to the conductance due to the voltage dependence of the barrier-penetration factor [see Eq. (C11)].

The omission of the **k** dependence of the self-energy (Appendix A 5) is probably the most serious simplification of the model. The dip in the calculated d^2I/dV^2 near $eV=-\hbar\omega_0$ is due to large **k** transfers in the self-energy, which are eliminated in a more realistic model. In Fig. 8, we show a calculation for statically screened polar coupling in which the $1/q^2$ factor in the vertex function effectively cuts off the large **k** transfers (Appendix A 3). As is apparent in Fig. 8, this cutoff substantially reduces the dip in reverse bias.

Also shown in Fig. 8 are experimental data for Au on n-CdS.[29] No attempt was made to describe the background accurately in this calculation, so the forward bias experimental curve has been shifted down for a comparison to the calculation. The value of α is approximately the appropriate value for CdS,[30] and the value of Γ_a was chosen to give the proper width. The agreement between the calculation and the experiment

[26] W. A. Harrison, Phys. Rev. **104**, 128 (1956).
[27] G. B. Wright and A. Mooradian, Phys. Rev. Letters **18**, 608 (1967).
[28] J. G. Adler and J. E. Jackson, Rev. Sci. Instr. **37**, 1049 (1966); R. T. Payne, Phys. Rev. **139**, A570 (1965).
[29] D. L. Losee (private communication).
[30] D. Berlincourt, H. Jaffe, and L. R. Shiozawa, Phys. Rev. **129**, 1009 (1963); W. S. Baer and R. N. Dexter, *ibid.* **135**, A1388 (1964); B. Tell, T. C. Damen, and S. P. S. Porto, *ibid.* **144**, 771 (1966).

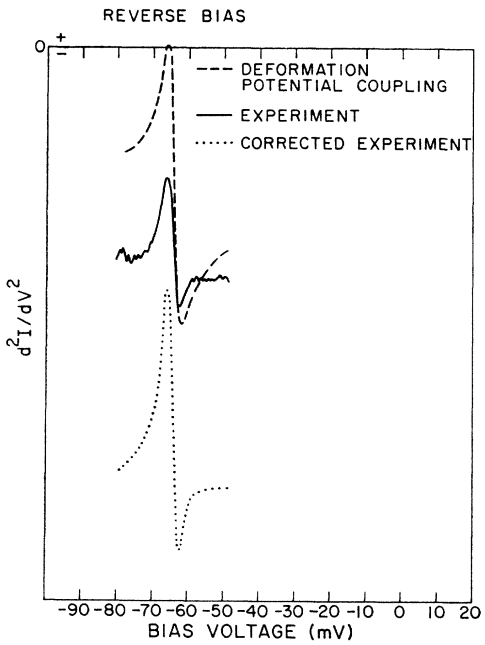

FIG. 7. Comparison of model calculation of Fig. 6 (dashed curve) to uncorrected experimental data of Fig. 6 (solid curve) and to experimental data with corrections (dotted curve) due to low-junction resistance in reverse bias (see Ref. 28). The strength of the experimental structure in reverse bias relative to the forward bias structure is in better agreement with the model calculation of Fig. 6 when these corrections are accounted for.

is reasonable. The rapid rise of the experimental curve of d^2I/dV^2 for $eV \gtrsim -\hbar\omega_0$ appears to be associated with a rising background (not accounted for in the calculation) instead of being due to the self-energy. The similarity of the results for statically screened polar coupling to the results for deformation potential coupling is evident upon comparison with Fig. 7.

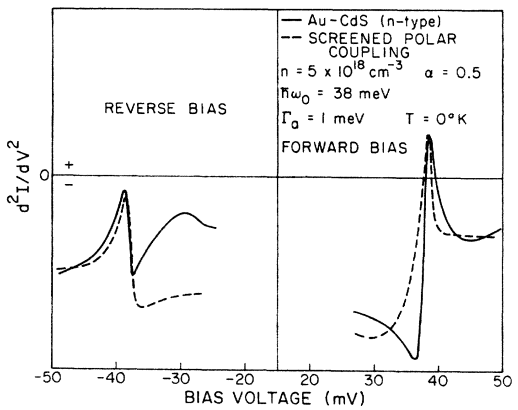

FIG. 8. The model calculation for statically screened polar coupling of electrons to optical phonons (Appendix A 3) is shown as dashed curve. Experimental data for Au on n-CdS (see Ref. 29) is shown as solid curve. Since no attempt was made to fit the background conductance, the forward bias experimental structure has been shifted for comparison to theory. The interesting feature of the calculation is the substantial reduction of the dip at $eV \gtrsim -\hbar\omega_0$ as compared with deformation-potential coupling. This reduction is due to cutting off the high momentum transfers in the self-energy. The expression for the self-energy used in this calculation is given by Eqs. (A3.7) and (A3.8) and, the barrier-penetration factor $D = D_0 \exp[-eV/2E_0 + \xi_q/E_0 - \hbar^2 k_{11}/2m^* E_0]$, where $E_0 = 375$ meV. Parameters used in this calculation are reasonably close to those appropriate to CdS (see Ref. 30).

We conclude that the influence of the optical-phonon interactions in the semiconductor electrode, via self-energy effects, on the tunneling conductance is the most convincing interpretation of the experimental observations in p-Si,[15,24] p-Ge,[25] n-CdS,[29] and GaAs[16,17] metal-semiconductor or metal-insulator-semicondcutor junctions. The approximate expressions for the self-energies used in this paper reproduce the qualitative features of the experimental data, but are not accurate enough to allow precision comparison to experimental data.

III. CONCLUSIONS

We have demonstrated explicitly that the alteration of the electronic states due to the interaction of electrons (holes) with the optical phonons in a degenerate semiconductor electrode of a tunnel junction (either metal-semiconductor or metal-insulator-semiconductor) can influence appreciably the tunneling conductance. These many-body effects in the semiconductor electrode manifest themselves in the tunneling conductance through the spectral weight $(1/\pi)\ \mathrm{Im}G^R(\xi_k,\epsilon)$ and, hence, through the self-energy $\Sigma(\mathbf{k},\epsilon)$. We have given analytic forms in second-order perturbation theory for deformation-potential coupling, statically screened polar coupling, and polar coupling to local-mode phonons. These simple forms are adequate to compare model calculations qualitatively to experiment, but more realistic expressions of the self-energy are needed for detailed comparison. For example, the influence of phonon dispersion and the existence of a maximum phonon wave vector must be accounted for in the self-energy due to deformation-potential coupling to optical phonons.

Experimental confirmation of these self-energy effects has been demonstrated most convincingly in the In-SiO_2-Si system[15,24] for which the data clearly shows an antisymmetric conductance (dI/dV) with respect to zero bias and a nearly symmetric curve of d^2I/dV^2. The symmetry of the line shapes with respect to zero bias is significant because it clearly distinguishes the structure due to self-energy effects associated with optical phonons from that expected for inelastic tunneling processes, such as phonon-assisted tunneling.[1,2,25] Owing to the threshold nature of inelastic tunneling, symmetric conductance (dI/dV) and antisymmetric d^2I/dV^2 are found, which is opposite to that found for the self-energy effects due to optical phonons.

The striking modification of the conductance of a tunnel junction in which one electrode is a degenerate semiconductor is due to two features: (a) The Fermi energy ζ is comparable to the phonon energy $\hbar\omega_0$ which results in large modifications of the spectral weight $(1/\pi)\ \mathrm{Im}G^R(\xi_k,\epsilon)$, and (b) the shape of the conductance

is dominated by phase-space restrictions in the semiconductor electrodes (i.e., the $\mathbf{k}_{\parallel}$ integration). It is, therefore, clear that any collective excitation of a degenerate semiconductor electrode can, in principle, be probed directly by tunneling. Such is the case for plasmons[18] and for acoustic phonons[31] in which the $\mathbf{k}$ dependence of the self-energy is important. This is to be contrasted to case of optical phonons where the ϵ dependence of the self-energy is the dominant feature. The observation of these self-energy effects provides a useful spectroscopic probe of the influence of elementary excitations in degenerate semiconductors because the line shapes are not strongly dependent upon the details of the barrier penetration factors or background conductance.

As discussed in Appendix B, the dependence of $\Lambda_{k,q}$ on $\mathbf{k}$ or $\mathbf{q}$, or equivalently the dependence of $D(\mathbf{k}_{\parallel},\xi_k,\xi_q)$ on ξ_k or ξ_q, is not well defined in the transfer-Hamiltonian model. In the discussion of self-energy effects in degenerate semiconductor electrodes, the ambiguity in $\Lambda_{k,q}$ is not significant, but in the case of metal electrodes, the observation of any self-energy effect (other than those due to the many-body density of states) depends critically on the ξ_k dependence of $D(\mathbf{k}_{\parallel},\xi_k,\xi_q)$, where ξ_k is the energy associated with the metal electrode in which the many-body interactions occur. This fact appears to us to constitute a serious flaw in previous analyses of metal-semiconductor contacts[17] and in more recent ones[21,22] of metal-insulator-metal junctions. We have avoided such difficulties by virtue of good fortune rather than by resolution of the underlying ambiguities associated with the transfer-Hamiltonian model. This resolution is an important prerequistie to the utilization of tunneling as a precision spectroscopic probe of electrode self-energy effects. Once it is achieved, however, the process of analyzing the experimental data in terms of model electronic self-energies can be reversed. An appropriate form of $D(\mathbf{k}_{\parallel},\xi_k,\xi_q)$ can be inserted in Eq. (1.7) [or Eq. (1.8) if D is independent of the bias], and this equation can be utilized to extract directly from the experimental d^2I/dV^2 the single-particle spectral weight $(1/\pi)\,\mathrm{Im}G^R(\xi_k,\epsilon)$.

Note added in proof. Some of the difficulties associated with the transfer-Hamiltonian model have been resolved recently.[31a] It has been shown that in the WKB approximation the exponential factor in the barrier penetration probability depends upon the energy variable ϵ, and not ξ_q or ξ_k. Since we have assumed that the left-hand electrode is noninteracting in the present work, $\epsilon=\xi_q-eV$. Therefore, because we have written the exponential factor in Eq. (2.5) in terms of ξ_q, and not ξ_k, the analysis in this paper is correct.

ACKNOWLEDGMENTS

The authors are indebted to Professor J. Bardeen for discussions of this mechanism for tunneling and to Professor W. D. Compton, D. Cullen, Dr. D. L. Losee, and Dr. F. Steinrisser for discussions of their data.

APPENDIX A: EVALUATION OF ELECTRONIC SELF-ENERGY

1. General Formulas

We confine our attention to expressions for the phonon-induced electronic proper self-energy given by second-order perturbation theory.[10] The diagrammatic expression for this contribution to the self-energy is shown in Fig. 4. In degenerate semiconductors typical phonon energies are of the same order of magnitude as the Fermi energy $\hbar\omega_{\mathrm{ph}}\sim\zeta$. Therefore, only the small value of the electron-phonon coupling constant permits us to restrict our consideration to the second-order expression shown in Fig. 4. In particular, vertex corrections cannot be shown to be small in a strong coupling model.[32]

We consider the interaction of electrons both with optical phonons, characteristic of the bulk semiconductor, and with local-mode phonons, characteristic of a light impurity in a lattice of heavier ions. A phenomenological model of the phonon propagator [i.e., the wavy line in Figs. 1, 2, and 4) is adopted in both cases. This propagator is given by

$$\mathfrak{D}(\mathbf{q},i\omega_q)=-2\hbar\omega_0/[\omega_q^2+(\hbar\omega_0)^2], \qquad \text{(A1.1)}$$

in which $\hbar\omega_0$ is the phonon energy. For optical phonons, in group-IV and -III–V semiconductors, typical phonon energies are $\hbar\omega_0\sim30$ meV and typical dispersion of the phonon energy across the Brillouin zone is $\Delta(\hbar\omega_0)\lesssim5$ meV. Therefore, the neglect of dispersion in the model phonon propagator leads to the consequence that the line shapes predicted in the tunnel characteristics are expected to be more sharp than those measured experimentally, especially for $eV\lesssim\hbar\omega_0$.

A free-carrier propagator,

$$\mathcal{G}_0(\mathbf{p},i\omega_p)=[i\omega_p-\xi_p]^{-1}, \qquad \text{(A1.2a)}$$

$$\xi_p=\hbar^2p^2/2m^*-\zeta, \qquad \text{(A1.2b)}$$

is used for the electronic propagator associated with the solid line in Fig. 4. In a model in which the electronic energy spectrum is taken to exhibit particle-hole symmetry, the substitution of the full propagator $\mathcal{G}$ in lieu of $\mathcal{G}_0$ in Fig. 4 causes no alteration of the expression for the self-energy Σ in the limit that $\Sigma(\mathbf{p},i\omega_p)$ depends only on $i\omega_p$.[33] However, the violation of particle-hole symmetry in degenerate semiconductors is the primary reason why the tunneling effect discussed in this paper

[31] H. J. Deuling (private communication).
[31a] J. A. Appelbaum and W. F. Brinkman (to be published); L. C. Davis (to be published).

[32] A. B. Migdal, Zh. Eksperim. i Teor. Fiz. 34, 1438 (1958) [English transl.: Soviet Phys.—JETP 7, 996 (1958)].
[33] S. Englesberg and J. R. Schrieffer, Phys. Rev. 131, 993 (1963).

is large. A solution of the integral equation obtained when $\mathcal{G}_0 \rightarrow \mathcal{G}$ in Fig. 4 has been considered elsewhere[34] in the case of deformation-potential electron-phonon interactions.

The characteristics of a model description of the electron-phonon interaction depend upon the nature of the chemical bonding in the semiconductor, its electronic energy-band structure, and the type of phonon under consideration. In the remaining parts of this appendix we specify various model interactions and their concomitant second-order electronic self-energies. This subappendix is concluded by a discussion of some general features of a phenomenological Fröhlich-type model[9] of the electron-phonon interaction.

The noninteracting electron-phonon Hamiltonian associated with Eqs. (A1.1) and (A2.2) is

$$\mathcal{H}_0=\sum_{\mathbf{k}} \xi_{\mathbf{k}} c_{\mathbf{k}}^{\dagger} c_{\mathbf{k}}+\hbar\omega_0 \sum_{\mathbf{q}} (b_{\mathbf{q}}^{\dagger} b_{\mathbf{q}}+\tfrac{1}{2}), \tag{A1.3}$$

in which $c_{\mathbf{k}}$ and $b_{\mathbf{q}}$ are the electron and phonon annihilation operators, respectively. The Fröhlich Hamiltonian is specified by assuming that the electron and phonon interact via an instantaneous interaction

$$\mathcal{H}_I=\sum_{\mathbf{k},\mathbf{q}} [V_{\mathbf{q}} b_{\mathbf{q}} c_{\mathbf{k}+\mathbf{q}}^{\dagger} c_{\mathbf{k}}+\text{H.c.}]. \tag{A1.4}$$

Using this model, the contribution to the retarded electronic self-energy shown in Fig. 4 is given by[10,20]

$$\Sigma(\mathbf{k},\epsilon)=\sum_{\mathbf{k}'} |V_{\mathbf{k}'-\mathbf{k}}|^2 \left\{ \frac{n(\xi_{\mathbf{k}'})+N(\hbar\omega_0)}{\epsilon+\hbar\omega_0-\xi_{k'}} - \frac{n(\xi_{\mathbf{k}'})-1-N(\hbar\omega_0)}{\epsilon-\hbar\omega_0-\xi_{k'}} \right\}, \tag{A1.5}$$

$$n(x)=[\exp(x/\kappa T)+1]^{-1}, \tag{A1.6a}$$

$$N(x)=[\exp(x/\kappa T)-1]^{-1}. \tag{A1.6b}$$

The first term in Eq. (A1.5) is the contribution to the self-energy due to (single) phonon absorption and the second term is that due to (single) phonon emission. Four properties of Eq. (A1.5) are significant. First, for low temperatures, $\kappa T \lesssim \hbar\omega_0$ (i.e., $T \lesssim 300°\text{K}$), $N(\hbar\omega_0) \cong \exp[-\hbar\omega_0/\kappa T] \rightarrow 0$ and, hence, its contribution in Eq. (A1.5) can be neglected. This approximation is made in all of the analyses given below. Second, $\text{Im}\Sigma(\mathbf{k},\epsilon)$ vanishes identically for all values of ϵ in the "quasiparticle window"

$$-\hbar\omega_0 < \epsilon < \hbar\omega_0 \tag{A1.7}$$

in the zero-temperature limit. Third, the abrupt increase in $\text{Im}\Sigma(\mathbf{k},\epsilon)$ to a finite value at $\epsilon=\pm\hbar\omega_0$ results in a logarithmic divergence in the real self-energy at this value of ϵ. This result remains true if $\mathcal{G}_0$ is replaced by $\mathcal{G}$ in Fig. 4 (the Hartree-Fock approximation for the self-energy). However, it does not remain valid if frequency-dependent vertex corrections[20] are introduced into Fig. 4 or if phonon dispersion is incorporated into the model.[18] Fourth, the $\mathbf{k}$ dependence of the self-energy is a consequence of the dependence of the electron-phonon vertex on $\mathbf{q}=\mathbf{k}-\mathbf{k}'$. If the $\mathbf{q}$ dependence of the vertex is weak, the self-energy will be almost independent of $\mathbf{k}$.[10,32]

[34] C. B. Duke and C. E. Swenberg (unpublished).

2. Deformation-Potential Hole-Phonon Coupling in Silicon and Germanium

The case of the deformation-potential coupling of holes to optical phonons in p-type silicon and germanium is described by use of the Fröhlich Hamiltonian.[23] The vertex $V_{\mathbf{q}}$ is specified by[23]

$$|V_{\mathbf{q}}|^2=\frac{E_{1,\text{op}}^2\hbar\omega_0}{2\Omega\rho v_s^2}\equiv\frac{K^2}{\Omega}, \tag{A2.1}$$

in which $E_{1,\text{op}}$ is an optical deformation-potential constant Ω is the crystal volume, ρ is the mass density of the crystal, and v_s is an average speed of sound in the crystal. The fact that the vertex function given by Eq. (A2.1) is a constant has the dual consequences that the sum over $\mathbf{k}'$ in Eq. (A1.5) can be performed analytically and that the electronic self-energy is essentially independent of $\mathbf{k}$. The expression for the self-energy at zero temperature already has been given[11]:

$$\begin{aligned}\Sigma_0(\epsilon)=&2K^2\theta(-\epsilon_+)\rho(-\epsilon_+)\tan^{-1}(-\zeta/\epsilon_+)^{1/2}\\ &-2K^2\theta(-\epsilon_-)\rho(-\epsilon_-)\tan^{-1}(-\zeta/\epsilon_-)^{1/2}\\ &+K^2\theta(\epsilon_+)\rho(\epsilon_+)\ln\left|\frac{\epsilon_+^{1/2}+\zeta^{1/2}}{\epsilon_+^{1/2}-\zeta^{1/2}}\right|\\ &-K^2\theta(\epsilon_-)\rho(\epsilon_-)\ln\left|\frac{\epsilon_-^{1/2}+\zeta^{1/2}}{\epsilon_-^{1/2}-\zeta^{1/2}}\right|\\ &-i\pi K^2\theta(\epsilon_+)\rho(\epsilon_+)\theta(-\hbar\omega_0-\epsilon)\\ &-i\pi K^2\theta(\epsilon_-)\rho(\epsilon_-)\theta(-\hbar\omega_0+\epsilon),\end{aligned} \tag{A2.2a}$$

$$\epsilon_{\pm}=\epsilon+\zeta\pm\hbar\omega_0, \tag{A2.2b}$$

$$\rho(\epsilon)=(2m^*/\hbar^2)^{3/2}(2\pi)^{-2}\epsilon^{1/2}. \tag{A2.2c}$$

These equations express those contributions to the self-energy which do not depend on the cutoff momentum q_c which must be imposed to limit the sum over $\mathbf{k}'$ in Eq. (A1.5) to a finite value. This cutoff is imposed by converting the sum over $\mathbf{k}'$ to an integral over $\xi_{k'}$ and taking the upper limit of the latter to be $E_D \gg \zeta$, $\hbar\omega_0$. The complete second-order expression for the self-energy is given by

$$\Sigma^{(2)}(\epsilon)=\Sigma_0(\epsilon)+\Sigma_D(\epsilon), \tag{A2.3a}$$

$$\Sigma_D(\epsilon)=-2K^2\rho(E_D)$$
$$+2K^2\theta(-\epsilon_-)\rho(-\epsilon_-)\tan^{-1}(-E_D/\epsilon_-)^{1/2}$$
$$+K^2\theta(\epsilon_-)\rho(\epsilon_-)\ln\left|\frac{E_D^{1/2}+\epsilon_-^{1/2}}{E_D^{1/2}-\epsilon_-^{1/2}}\right|. \quad \text{(A2.3b)}$$

The complete expression for $\Sigma^{(2)}(\epsilon)$ given by Eq. (A2.3), in which Σ_0 is specified by Eq. (A2.2), satisfies all of the appropriate sum rules and limits. The second term of Eq. (A2.3b) is incorporated into numerical calculations of the self-energy according to

$$\Sigma_{\rm num}(\epsilon)=\Sigma_0(\epsilon)+\pi K^2\theta(-\epsilon_-)\rho(-\epsilon_-). \quad \text{(A2.4)}$$

The logarithmic singularities in the real part of the self-energy at $\epsilon=\pm\hbar\omega_0$ (i.e., $\epsilon_\pm=\zeta$) are evident from Eq. (A2.2). In an actual semiconductor, these singularities do not occur because the holes have a finite lifetime due to their interaction with impurities and acoustical phonons[23] even in the absence of their interaction with optical phonons. This effect is simulated in numerical calculations of the tunneling line shape by making the replacement

$$\ln|\zeta^{1/2}-\epsilon_\pm^{1/2}|\rightarrow\tfrac{1}{2}\ln[(\zeta^{1/2}-\epsilon_\pm^{1/2})^2+\Gamma_\pm^2/4\zeta] \quad \text{(A2.5a)}$$

in the real part of the singular terms in Eqs. (A2.2) and (A2.4), and

$$\pi\theta(-\hbar\omega_0\pm\epsilon)\rightarrow\tfrac{1}{2}\pi+\tan^{-1}[(-\hbar\omega_0\pm\epsilon)/\Gamma_\pm] \quad \text{(A2.5b)}$$

in the imaginary part of $\Sigma_0(\epsilon)$ in Eqs. (A2.2) and (A.24). The widths $\Gamma_\pm$ of the peaks in the real part of the self-energy are taken as adjustable parameters used to incorporate the influence of the other mechanisms causing finite-hole lifetimes. The form of Eq. (A2.5) is chosen so that the logarithmic divergence is that associated with an energy variable $\epsilon\rightarrow\pm\hbar\omega_0+i\Gamma_\pm$ at the two divergences. Evidently $\Gamma_+\neq\Gamma_-$ in general, although for numerical calculations we use

$$\Gamma_+=\Gamma_-\equiv\Gamma_a. \quad \text{(A2.6)}$$

[To be complete, we also add to $\Sigma_{\rm num}(\epsilon)$, in Eq. (A2.4), the term $-i\Gamma_a$.]

Finally, we note that Eq. (A2.2) reduces to that obtained by Engelsberg and Schrieffer[33] in the limit that all terms are expanded in powers of $(\epsilon_\pm-\zeta)/\zeta$ and only the leading terms are retained. This particle-hole symmetry limit is not applicable for the description of degenerate semiconductors used as tunnel-junction electrodes because in this doping range $\hbar\omega_0\sim\zeta$. However, for many of these semiconductors $\hbar\omega_0\lesssim1.5\zeta$ and, hence, only the divergent logarithmic terms in Eq. (A2.2) contribute to $\Sigma(\epsilon)$ in the region of interest (i.e., $\epsilon\lesssim\hbar\omega_0$).

3. Polar Electron-Optical-Phonon Coupling

The interaction between electrons and optical phonons has been studied extensively[35] using the Fröhlich Hamiltonian and the interaction[36]

$$V_q^{(0)}=\left[\frac{4\pi\alpha}{\Omega q^2}\left(\frac{\hbar}{2m^*\omega_0}\right)^{1/2}\right]^{1/2}\hbar\omega_0, \quad \text{(A3.1a)}$$

$$\alpha=e^2\left(\frac{m^*}{2\omega_0\hbar^3}\right)^{1/2}\left(\frac{1}{\epsilon_\infty}-\frac{1}{\epsilon_0}\right), \quad \text{(A3.1b)}$$

in which ϵ_0 is the static and ϵ_∞ is the optical dielectric constant of the semiconductor. The second-order self-energy for both intrinsic[35] and degenerate[20] semiconductors has been evaluated using Eq. (A3.1). The self-energy calculated using Eq. (A3.1) exhibits[20] two additional divergences to those at $|\epsilon|=\pm\hbar\omega_0$ resulting from a deformation-potential interaction. The q^{-2} divergence in Eq. (A2.1a) leads to a divergence in the real part of $\Sigma(\mathbf{k},\epsilon)$ at $k=k_F$. The imaginary part of $\Sigma(\mathbf{k},\epsilon)$ diverges for $\epsilon=\xi_k-\hbar\omega_0$ if the two conditions

$$-\hbar\omega_0-\zeta<\epsilon<-\hbar\omega_0,\quad k<k_F \quad \text{(A3.2a)}$$

are satisfied and for $\epsilon=\xi_k+\hbar\omega_0$ if the conditions

$$\epsilon>\hbar\omega_0,\quad k>k_F \quad \text{(A3.2b)}$$

are satisfied. Primarily because of these divergences, the $\mathbf{k}$ dependence of the self-energy is significant[20] for the unscreened polar electron-phonon coupling given by Eq. (A3.1) and for electron-plasmon interactions.[18]

If free carriers are present in a semiconductor, the Fröhlich Hamiltonian is no longer adequate to describe the electron-phonon system in the presence of polar coupling. The electron-electron interactions must be included in the model Hamiltonian. However, analyses[37,38] of this extended Hamiltonian in the random-phase approximation indicate that a diagram of the form shown in Fig. 4 still contributes to the electronic proper self-energy provided one defines the vertex function to be

$$V(\mathbf{q},i\omega_q)=V_q^{(0)}/\epsilon(\mathbf{q},i\omega_q), \quad \text{(A3.3)}$$

in which $\epsilon(\mathbf{q},i\omega_q)$ is the dynamic dielectric function characterizing the electron fluid. Mahan and Duke[20] have studied the second-order contribution to the electronic self-energy using the vertex given by Eq. (A3.3). They found that both the divergence in the real part of $\Sigma(\mathbf{k},\epsilon)$ at $k=k_F$ and the divergences in its imaginary part at $\epsilon=\xi_k\pm\hbar\omega_0$ disappear when the general vertex given by Eq. (A3.3) is used in the analysis.

In order to perform an analysis of the tunneling characteristics, it is possible to utilize a simple model of the dielectric function (e.g., static screening[20]) and

[35] See, e.g., G. Whitfield and R. Puff, Phys. Rev. **139**, A338 (1965), and references therein.
[36] H. Frölich, H. Pelzer, and S. Zienau, Phil. Mag. **41**, 221 (1950).
[37] A. Ron, Phys. Rev. **132**, 978 (1963).
[38] J. R. Schrieffer, *Theory of Superconductivity* (W. A. Benjamin, Inc., New York, 1964), Chap. 6.

evaluate $\Sigma(\mathbf{k},\epsilon)$ exactly. However, the quantity of most interest is the $\mathbf{k}$ dependence of the remaining singularity in $\Sigma(\mathbf{k},\epsilon)$ at $\epsilon=\pm\hbar\omega_0$. Therefore, it is convenient to review a few of the considerations given by Mahan and Duke[20] which lead to a simplified formula for this divergent contribution to the self-energy.

When the dynamic vertex given by Eq. (A3.3) is used in Fig. 4, the self-energy at zero temperature is given by[20]

$$\Sigma(\mathbf{k},\epsilon)=\Sigma_{\rm ph}(\mathbf{k},\epsilon)+\Sigma_F(\mathbf{k},\epsilon)+\Sigma_r(\mathbf{k},\epsilon)\,, \tag{A3.4a}$$

$$\Sigma_{\rm ph}(\mathbf{k},\epsilon)=\sum_{\mathbf{q}}|V_{\mathbf{q}}^{(0)}|^2\,{\rm Re}\left[\frac{1}{\epsilon^2(\mathbf{q},-\hbar\omega_0)}\right]\times\frac{1}{\epsilon-\xi_{\mathbf{k}+\mathbf{q}}-\hbar\omega_0}\,, \tag{A3.4b}$$

$$\Sigma_F(\mathbf{k},\epsilon)=-\sum_{\mathbf{q}}|V_{\mathbf{q}}^{(0)}|^2\epsilon^{-2}(\mathbf{q},\epsilon-\xi_{\mathbf{k}+\mathbf{q}})n(\xi_{\mathbf{k}+\mathbf{q}})\times[(\epsilon-\xi_{\mathbf{k}+\mathbf{q}}-\hbar\omega_0)^{-1}-(\epsilon-\xi_{\mathbf{k}+\mathbf{q}}+\hbar\omega_0)^{-1}]. \tag{A3.4c}$$

The contribution $\Sigma_r(\mathbf{k},\epsilon)$ is due to the cuts and poles of $\epsilon^{-2}(\mathbf{q},i\omega_p)$. It was analyzed in Ref. 20 and causes no phonon-induced singularities in the self-energy so we do not consider it further. If $\epsilon(\mathbf{q},i\omega_q)$ is taken in the static approximation to be real and independent of $i\omega_q$, then $\Sigma_{\rm ph}$ and Σ_F combine in Eq. (A3.4) to yield an expression identical to the Fröhlich-model result given by Eq. (A1.5). It should be noted that the combination of $\Sigma_{\rm ph}$ and Σ_F always occurs for the contribution to the self-energy due to the pole of the $(\epsilon-\xi_{\mathbf{k}+\mathbf{q}}-\hbar\omega_0)^{-1}$ factor. This combination is important because it is responsible for the quasiparticle window in the energy range $-\hbar\omega_0<\epsilon<\hbar\omega_0$, at zero temperature. It does not occur in a model in which dynamic screening is utilized.

Using the static dielectric function

$$\epsilon(\mathbf{q},0)=1+(k_s/q)^2\,, \tag{A3.5a}$$

$$k_s^2=6\pi ne^2/\zeta\epsilon_0\,, \tag{A3.5b}$$

in Eq. (A3.4), the electronic proper self-energy becomes

$$\Sigma(\mathbf{k},\epsilon)=\Sigma_h(\mathbf{k},\epsilon)+\Sigma_e(\mathbf{k},\epsilon)\,, \tag{A3.6a}$$

$$\Sigma_h(\mathbf{k},\epsilon)=\frac{\hbar^2}{m^*}\int_0^{k_F}\frac{q\,dqG(k,q)}{\epsilon-\xi_q+\hbar\omega_0}\,, \tag{A3.6b}$$

$$\Sigma_e(\mathbf{k},\epsilon)=\frac{\hbar^2}{m^*}\int_{k_F}^{\infty}\frac{qdqG(k,q)}{\epsilon-\xi_q-\hbar\omega_0}\,, \tag{A3.6c}$$

$$G(k,q)=\frac{\alpha\hbar\omega_0}{4\pi}\left(\frac{\hbar\omega_0}{\xi_k+\zeta}\right)^{1/2}\left\{\frac{k_s^2}{k_s^2+(k+q)^2}-\frac{k_s^2}{k_s^2+(k-q)^2}+\ln\left[\frac{k_s^2+(k+q)^2}{k_s^2+(k-q)^2}\right]\right\}. \tag{A3.6d}$$

Although the integrals in Eq. (A3.6) can be performed analytically, the singularities in $\Sigma(\mathbf{k},\epsilon)$ occur because of the $(\epsilon-\xi_q\pm\hbar\omega_0)^{-1}$ factors at the endpoints of the integrations.[39] Those terms contributing singularities at the edge of the quasiparticle window are given by

$${\rm Re}\Sigma_{\rm sing}(k,\epsilon)=G(k,k_F)\,\ln\left|\frac{\hbar\omega_0-\epsilon}{\hbar\omega_0+\epsilon}\right|\,, \tag{A3.7a}$$

$$g_\pm(k,\epsilon)=G[k,\,q=(2m^*\epsilon_\pm/\hbar^2)^{1/2}], \tag{A3.7b}$$

$${\rm Im}\Sigma(k,\epsilon)=-i\pi[g_+(k,\epsilon)\theta(-\hbar\omega_0-\epsilon)\theta(\epsilon_+)+g_-(k,\epsilon)\theta(-\hbar\omega_0+\epsilon)], \tag{A3.7c}$$

$$\epsilon_\pm=\epsilon+\zeta\pm\hbar\omega_0\,. \tag{A3.7d}$$

As in the deformation-potential coupling calculations (Appendix A 2), the effect of the finite lifetime of the electrons (holes) is simulated by making the replacements

$$\ln|\hbar\omega_0\pm\epsilon|\rightarrow\tfrac{1}{2}\ln[(\hbar\omega_0\pm\epsilon)^2+\Gamma_a^2], \tag{A3.8a}$$

$$\pi\theta(-\hbar\omega_0\pm\epsilon)\rightarrow\tfrac{1}{2}\pi+\tan^{-1}[(-\hbar\omega_0\pm\epsilon)/\Gamma_a], \tag{A3.8b}$$

$$\Sigma(\mathbf{k},\epsilon)\rightarrow\Sigma(\mathbf{k},\epsilon)-i\Gamma_a\,, \tag{A3.8c}$$

where Γ_a is an adjustable parameter. Equation (A3.7a) is identical to an interpolation formula for $\Sigma(\mathbf{k},\epsilon)$ given by Conely and Mahan (CM)[17] (corrected for a sign error in the third term). Their analysis of the tunneling line shape is recovered by making the further approximation

$$q_\pm(k)\rightarrow g_\pm(k_F)\,. \tag{A3.9}$$

Comparison of Eqs. (A3.7) and (A3.9) with Eq. (A2.2) indicates that their approximations render the CM analysis[17] of polar coupling identical to an approximate analysis of deformation-potential coupling in which the lifetime of the electron is set arbitrarily to infinity and the logarithmic terms in Eq. (A2.2) are evaluated in the limit of particle-hole summetry[33] (see Appendix A 2).

4. Polar Coupling to Local-Mode Phonons

The single-Boson propagator for a localized vibronic mode is identical to that given by Eq. (A.11) in which $\hbar\omega_0$ is taken to be the energy of the local mode. Our interest in these modes is motivated by the observation of the localized mode associated with boron impurities in silicon in tunneling[15] as well as infrared absorption[40] measurements. In this case, we can estimate the electron-localized-mode coupling in degenerate silicon by using a model in which the boron impurity is treated as a harmonically oscillating point charge in a degenerate hole (electron) fluid. The vertex function resulting from

[39] J. Tarski, J. Math. Phys. 1, 149 (1960).
[40] M. Balkanski and W. Nazarewicz, J. Phys. Chem. Solids 27, 671 (1965).

such a model is given by

$$|V_q(i\omega_q)|^2=n_i\frac{(4\pi e^2)^2}{\Omega q^2}\frac{\hbar}{M_i\omega_0}\frac{1}{\epsilon^2(\mathbf{q},i\omega_q)}, \quad \text{(A4.1)}$$

in which n_i is the concentration and M_i is the mass of the (charged) impurity. The associated second-order electronic proper self-energy is obtained by use of (A1.1) for the propagator and (A4.1) for the vertex in Fig. 4.

A comparison of Eq. (A4.1) with Eqs. (A3.1) and (A3.3) indicates that the bulk hole–local-mode coupling in silicon is essentially identical in form to the polar hole–LO-phonon coupling in a polar semiconductor. The scaling of the vertex function with $n_i^{1/2}$ is in qualitative agreement with the observations of Wolf.[15] The quantiative expressions for the self-energy can be obtained from Appendix A 4 by making the identification

$$\alpha_i=\frac{4\pi e^4 n_i}{(\hbar\omega_0)^2}\left(\frac{\hbar}{M_i\omega_0}\right)\left(\frac{2m^*\omega_0}{\hbar}\right)^{1/2} \quad \text{(A4.2)}$$

in the expressions for the self-energy.

5. Influence of Maximum Phonon Wave Vector and of Phonon Dispersion

The influence on the electronic self-energy of the existence of a maximum phonon wave vector and of phonon dispersion, i.e.,

$$\hbar\omega(\mathbf{q})=\hbar\omega_0-\alpha q^2, \quad \text{(A5.1)}$$

may be investigated by writing Eq. (A1.5) as

$$\Sigma(\mathbf{k},\epsilon)=\Sigma_+(\mathbf{k},\epsilon)+\Sigma_-(\mathbf{k},\epsilon), \quad \text{(A5.2a)}$$

$$\Sigma_+(\mathbf{k},\epsilon)=\frac{m\Omega}{8\pi^2\hbar^2 k}\int_{-\zeta}^{\infty}d\xi_{k'}n(\xi_{k'})\times\int_{(k-k')^2}^{q_m^2}\frac{|V(x)|^2dx}{\epsilon+\hbar\omega_0-\xi_{k'}-\alpha x}, \quad \text{(A5.2b)}$$

$$\Sigma_-(\mathbf{k},\epsilon)=\frac{m\Omega}{8\pi^2\hbar^2 k}\int_{-\zeta}^{\infty}d\xi_{k'}n(-\xi_{k'})\times\int_{(k-k')^2}^{q_m^2}\frac{|V(x)|^2dx}{\epsilon-\hbar\omega_0-\xi_{k'}+\alpha x}, \quad \text{(A5.2c)}$$

$$q_m^2=\min[(k+k')^2,\ q_c^2]. \quad \text{(A5.2d)}$$

We have used q_c to denote the maximum phonon wave vector and have assumed $\hbar\omega(q_c)/\kappa T\gg 1$. Our previous results for the deformation potential [Eq. (A2.2)] are recovered if $q_c^2>(k+k')^2$, $\alpha=0$, and $|V(x)|^2=K^2/\Omega$.

The occurrence of phonon dispersion removes the logarithmic singularity in the self-energy at $\epsilon=\pm\hbar\omega_0$ and spreads the peaks in $\Sigma(\mathbf{k},\epsilon)$ over a range of ϵ values from $\hbar\omega(q_c)$ to $\hbar\omega_0$, as found for electron-plasmon interactions.[18,41,42] The finite value of q_c^2 influences primarily $\Sigma_-(\mathbf{k},\epsilon)$, in which case it substantially reduces the magnitude of the self-energy for $k\gtrsim q_c$. This result was artificially inserted in Appendix A 2 by introducing an upper limit on the integral over $\xi_{k'}$. However, the restriction is on the value of $\mathbf{k}$, not ϵ. This fact has the consequence that the contributions to the tunneling line shapes involving large $\mathbf{k}$ electrons are modified from the predictions of the model developed in Appendix A 2.

For deformation-potential interactions the imaginary part of $\Sigma(\mathbf{k},\epsilon)$ can be evaluated exactly as the sum of two arc lengths in the k'-x plane.[18] The x integrations for the real part yield

$$I_\pm(k,k',\epsilon)=\pm\frac{k^2}{\Omega\alpha}\ln\left[\frac{\epsilon-\xi_{k'}\pm\hbar\omega(k-k')}{\epsilon-\xi_{k'}\pm\hbar\omega(q_m)}\right]. \quad \text{(A5.3)}$$

At $T=0$ the subsequent k' integration in Eq. (A1.2) also can be performed analytically in terms of elementary functions [although careful attention must be paid to the limits due to both Eq. (A5.2d) and the exclusion-principle restrictions]. These calculations have been carried out and the resulting expressions evaluated numerically leading to the results stated in the previous paragraph. In numerical calculations of the tunnel characteristics we usually use the simpler self-energies developed in Appendix A 2 in order to reduce the computation time.

APPENDIX B: TRANSFER-HAMILTONIAN FORMALISM

In this appendix, we discuss some of the difficulties inherent in the transfer-Hamiltonian formalism. For clarity, let us repeat Eq. (1.7) for the tunneling current:

$$I=\frac{4\pi e}{\hbar}\sum_{\mathbf{k},\mathbf{q}}|\Lambda_{\mathbf{k},\mathbf{q}}|^2\int_{-\infty}^{+\infty}d\epsilon[f(\epsilon)-f(\epsilon+eV)]\times\delta(\epsilon-\xi_q+eV)\frac{1}{\pi}\mathrm{Im}G^R(\xi_k,\epsilon).$$

In a noninteracting-electron model of the semiconductor electrode,

$$\pi^{-1}\,\mathrm{Im}G^R(\xi_k,\epsilon)=\delta(\xi_k-\epsilon). \quad \text{(B1)}$$

This has the consequence that for any initial state $|\mathbf{q}\rangle$ on the left, there is only one possible final state $|\mathbf{k}\rangle$ on the right consistent with the conservation of energy and specular reflection ($\mathbf{k}_{||}$ conservation):

$$\mathbf{k}_{||}=\mathbf{q}_{||}, \quad \xi_k=\xi_q-eV. \quad \text{(B2)}$$

(Specification of $\mathbf{k}_{||}$ and ξ_k is equivalent to specifying $\mathbf{k}$.) We refer to $\Lambda_{k,q}$ for such a pair of states related by conservation of energy and $\mathbf{k}_{||}$ in the noninteracting

[41] L. Hedin, B. I. Lundqvist, and S. Lundqvist, Solid State Commun. 5, 237 (1967).

[42] B. I. Lundqvist, Phys. Kondensienten Materie 6, 193 (1967); 6, 206 (1967).

model as a diagonal element. Similar considerations apply for transfer from right to left.

When many-body interactions are present, $\mathbf{k}_{\parallel}$ and the total energy ϵ are given conserved. However, the term

$$\frac{1}{\pi}\mathrm{Im}G^R(\xi_{\mathbf{k}},\epsilon)=\frac{(1/\pi)\,\mathrm{Im}\Sigma(\xi_{\mathbf{k}},\epsilon)}{[\xi_{\mathbf{k}}-\epsilon+\mathrm{Re}\Sigma(\xi_{\mathbf{k}},\epsilon)]^2+\mathrm{Im}^2\Sigma(\xi_{\mathbf{k}},\epsilon)}\,, \tag{B3}$$

which appears in Eq. (1.7), has the consequence that for each initial state $|\mathbf{q}\rangle$, which has total energy ϵ, the tunneling electron can make a transition to any final state $|\mathbf{k}\rangle$ of arbitrary $\xi_{\mathbf{k}}$ (but with $\mathbf{k}_{\parallel}=\mathbf{q}_{\parallel}$). The most weight according to (B3) is then given to those states with $\xi_{\mathbf{k}}\simeq\xi(\epsilon)$, where

$$\xi(\epsilon)-\epsilon+\mathrm{Re}\Sigma(\xi(\epsilon),\epsilon)=0\,. \tag{1.9'}$$

Not only does the most probable final state have an energy $\xi(\epsilon)$ different from that of the noninteracting case ($\xi_{\mathbf{k}}=\epsilon$), but also there is in general a spread of energies about $\xi(\epsilon)$ which are possible final-state energies. Therefore, the electrode interactions probe the off-diagonal elements of $\Lambda_{\mathbf{k},\mathbf{q}}$.

These off-diagonal elements are not well defined. For instance, if we were to use the expression[4]

$$\Lambda_{\mathbf{k},\mathbf{q}}=-i\hbar\langle\mathbf{k}|J|\mathbf{q}\rangle\,, \tag{B4}$$

where J is the current operator, we would find that this expression is not position-independent for the off-diagonal elements. If we were to use a more general expression[4]

$$\Lambda_{\mathbf{k},\mathbf{q}}=\langle\mathbf{k}|H-W_{\mathbf{k},\mathbf{q}}|\mathbf{q}\rangle\,, \tag{B5}$$

we would find that $\Lambda_{\mathbf{k},\mathbf{q}}\neq\Lambda_{\mathbf{q},\mathbf{k}}^*$ for the off-diagonal elements. Such non-Hermitian character follows from the nonorthogonality of the basis functions.

The problem of determining the matrix elements $\Lambda_{\mathbf{k},\mathbf{q}}$ has been considered by several authors.[6,43,44] For example, Schmid[44] asserts that

$$|\Lambda_{\mathbf{k},\mathbf{q}}|^2\propto e^{-\eta_L-\eta_R}, \tag{B6a}$$

where (in our notation)

$$\eta=\int_0^b\left[\frac{2m_b}{\hbar^2}\left(\phi(x)-\xi_{\mathbf{q}}+\frac{\hbar^2k_{\parallel}^2}{2m^*}+eV\right)\right]^{1/2}dx \tag{B6b}$$

and

$$\eta_R=\int_0^b\left[\frac{2m_b}{\hbar^2}\left(\phi(x)-\xi_{\mathbf{k}}+\frac{\hbar^2k_{\parallel}^2}{2m^*}\right)\right]^{1/2}dx. \tag{B6c}$$

The effective mass in the barrier is m_b, the potential is $\phi(x)$, and the width is b. These expressions follow from the particular choice for the basis functions made in Ref. 45. An objection to these basis functions is that the symmetry, present when $V=0$, is broken when $V\neq0$, the case that must be considered if current is flowing.

The prefactors usually are well defined in terms of phase-space variables on one side of the junction or the other side. It is the energy variable which appears in the WKB exponent which is uncertain.

In the analysis of the influence of phonons in a normal metal upon the tunneling current,[21] an expression such as (B6), in which appears the energy variable of the side in which the interactions take place, is essential for there to be any effect. For the experiments discussed in this paper, however, this is not the case.

In metal-semiconductor and metal-insulator-semiconductor junctions, the phase-space integral

$$\int\frac{d^2k_{\parallel}}{(2\pi)^2}D(\mathbf{k}_{\parallel},\xi_{\mathbf{k}},\xi_{\mathbf{q}})$$

is the principal factor in determing the shape of dI/dV.[13] The available area in phase space, $(2\pi m^*/\hbar^2)(\xi_{\mathbf{k}}+\zeta)$, is the most important quantity, and not the variations of D with $\mathbf{k}_{\parallel}$, $\xi_{\mathbf{k}}$, $\xi_{\mathbf{q}}$, or eV, which are small.

In our original letter,[11] we (arbitrarily) chose to write D as $D(\mathbf{k}_{\parallel},\xi_{\mathbf{k}})$, where

$$D(\mathbf{k}_{\parallel},\xi_{\mathbf{k}})=D(\mathbf{k}_{\parallel},\xi_{\mathbf{k}},\xi_{\mathbf{q}}=\xi_{\mathbf{k}}+eV)\,. \tag{B7}$$

That is, we have approximated the off-diagonal elements of $\Lambda_{\mathbf{k},\mathbf{q}}$ (for fixed $\mathbf{k}_{\parallel}$, $\xi_{\mathbf{k}}$) by a diagonal element. This approximation has two disadvantages. (1) It superficially appears that the $\xi_{\mathbf{k}}$ of $D(\mathbf{k}_{\parallel},\xi_{\mathbf{k}})$ is responsible for the observed effect, whereas the effect is primarily caused by the alteration of the available area in phase space due to self-energy effects. (2) For certain models of D, the extremely high momentum transfers cause an unphysical divergence in the conductance for $|eV|>\hbar\omega_0$ unless the associated integrals are arbitrarily cut off at some point.

In this paper, we shall approximate the off-diagonal elements by a different diagonal element

$$D(\mathbf{k}_{\parallel},\xi_{\mathbf{q}})=D(\mathbf{k}_{\parallel},\xi_{\mathbf{k}}=\xi_{\mathbf{q}}-eV,\xi_{\mathbf{q}})\,. \tag{B8}$$

Since the electrons on the left are noninteracting,

$$\xi_{\mathbf{q}}=\epsilon+eV\,. \tag{B9}$$

Hence, we have written the barrier penetration factor in terms of the two quantities conserved across the junction, ϵ and $\mathbf{k}_{\parallel}$. The choice (B8) is, of course, arbitrary, but it is not subject to the difficulties (1) and (2) discussed above. In addition, for metal-semiconductor and metal-insulator-semiconductor, this choice does treat the principal effect (alteration of the available phase space) properly.

In Fig. 9, we show a comparison of d^2I/dV^2 calculated for the two approximations (B7) and (B8) for a simple model barrier penetration factor and deformation-

[43] R. E. Prange, Phys. Rev. 131, 1083 (1963).
[44] A. Schmid, Z. Physik 205, 35 (1967).
[45] B. E. Deal, E. H. Snow, and C. A. Mead, J. Phys. Chem. Solids 27, 1873 (1966).

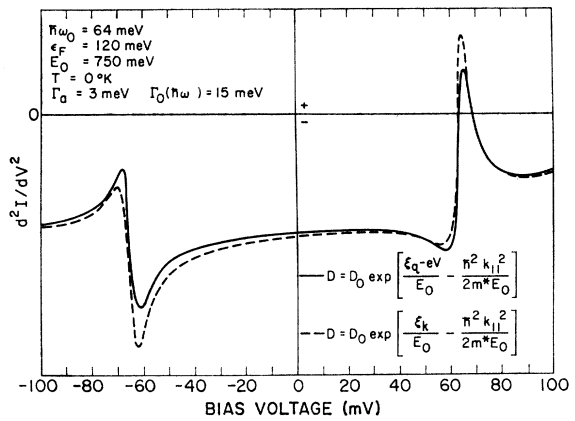

FIG. 9. Calculation of d^2I/dV^2 versus V for deformation-potential coupling for two approximate forms of the barrier-penetration factor [see Eqs. (B7) and (B8)]. The solid corresponds to the choice of writing D in terms of the two quantities conserved across the junction, $\xi_q = \epsilon + eV$ and $\mathbf{k}_{||}$ (see Appendix B). The dashed curve corresponds to the choice made in Ref. 11. The self-energy is given by Eqs. (A2.2)–(A2.6).

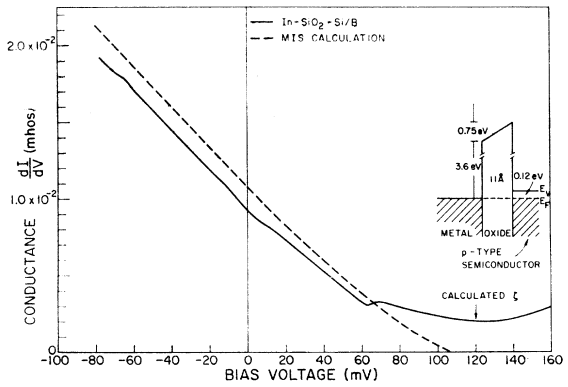

FIG. 10. Numerical calculation of the one-electron conductance of a metal-insulator-semiconductor junction is shown as dashed curve. The barrier-penetration factor is given by Eq. (C2) and the current is given by Eq. (C1). Solid curve is experimental data for p-Si (Ref. 24).

potential coupling. Each calculation was carried 30 Γ's off the energy shell

$$\xi(\epsilon) - 30\Gamma < \xi_k < \xi(\epsilon) + 30\Gamma, \tag{B10}$$

where

$$\Gamma = \Gamma_0(\hbar\omega_0) + \Gamma_a. \tag{B11}$$

The two curves are qualitatively similar, except that we see that the choice (b) emphasized the off-energy-shell integration or lifetime effects more than choice (a) for $|eV| > \hbar\omega_0$. This result occurs because these off-energy-shell integrations contribute to dI/dV in the same manner as a threshold effect which gives a step up in the conductance for $|eV| > \hbar\omega_0$ and a peak up (down) in d^2I/dV^2 at $eV = +\hbar\omega_0(-\hbar\omega_0)$.

In conclusion, we observe that it has not yet been demonstrated unambiguously (either theoretically or experimentally) that many-body effects in the electrodes have altered the tunnel current through the energy variable appearing in the WKB exponent in D. All junctions[15–17,25,29] in which electrode self-energy effects due to optical phonons have been observed clearly are those in which the phase-space factors can account for the qualitative features of the observations.

APPENDIX C: METAL-INSULATOR-SEMICONDUCTOR BARRIER-PENETRATION FACTOR

To accurately analyze the structure in the experimental d^2I/dV^2 curves resulting from the electronic self-energy effects, it is necessary to have a model of the barrier-penetration factor and, hence, an understanding of the one-electron or background conductance. Also, it is convenient to have a simple form or model of the barrier-penetration factor that permits accurate line shape analysis. In this appendix, we describe how such a model may be found from considerations of the more detailed numerical calculations of the one-electron conductance.

It has been shown that for metal electrodes deposited upon vacuum-cleaved n-Ge,[25] the calculations of the Schottky-barrier tunnel conductance[46] adequately describe the shape and the magnitude of the conductance-versus-bias curves. The observation of the self-energy effects due to deformation-potential hole-phonon coupling has, however, been in air-cleaved heavily doped p-type Si [15,24] and Ge.[25] The local-mode phonon coupling has been seen only in the Si junctions.[15,24] The simple Schottky-barrier calculations are invalid for the Si junctions because both the vacuum-cleaved samples, and the Schottky-barrier calculations indicate that intimate metal-semiconductor contacts on such heavily doped Si behave essentially as electrical shorts. Such low resistance is the result of a low barrier height[47] and high doping levels ($\sim 10^{20}$ cm^{-3}). Therefore, in these junctions it was necessary to take into account the insulating layer formed on the Si surface due to air cleavage. The nature of the barrier in the p-type Ge junctions which are cleaved in air is not known

In Fig. 10, we show a comparison of the data for In data deposited on air-cleaved B-doped Si [24] with a numerical calculation of the conductance of a metal-insulator-semiconductor (MIS) junction in which the tunneling takes place through a thin insulating layer with a high potential barrier. Parameters for the barrier heights were chosen to agree with typical barrier heights for thick (500 Å) thermally grown oxides ($\phi_M = 3.6$ eV, $\phi_S = 4.35$ eV).[45] The electron effective mass in the barrier, m_b, was taken to be 0.47 m_0 [48] and the thickness $b = 11$ Å was chosen to give the proper magnitude of dI/dV for the measured contact area

[46] J. W. Conley, C. B. Duke, G. D. Mahan, and J. J. Tiemann, Phys. Rev. **150**, 466 (1966).
[47] C. A. Mead and W. A. Spitzer, Phys. Rev. Letters **10**, 471 (1963).
[48] E. H. Snow, Solid State Commun. **5**, 813 (1967).

$A=4.5\times10^{-5}$ cm^2. For these highly doped samples, field penetration into the semiconductor was found to be unimportant and was neglected. The contributions to the conductance of both the light hole band and the heavy hole band, but not the split-off band, were included in the calculation.

The current for the light (heavy) hole band was calculated from[49]

$$I=\frac{2eA}{\hbar}\int d\epsilon[f(\epsilon-eV)-f(\epsilon)]\int\frac{d^2k_{\parallel}}{(2\pi)^2}D(\mathbf{k}_{\parallel},\xi_k), \quad \text{(C1)}$$

where

$$D(\mathbf{k}_{\parallel},\xi_k)=16\frac{v_{Rx}}{v_{Lx}}\frac{K(0)}{K(b)}\left\{\left[\exp\left(-2\int_0^b K(x)dx\right)\right]\Big/\left[1+\left(\frac{m_bk}{m^*K(b)}\right)^2\right]\left[1+\left(\frac{m_LK(0)}{k_{FL}m_b}\right)^2\right]\right\}, \quad \text{(C2a)}$$

$$K(x)=\left[\frac{2m_b}{\hbar^2}\left(\phi(x)+\xi_k+\frac{\hbar^2k_{\parallel}^2}{2m_b}\right)\right]^{1/2}, \quad \text{(C2b)}$$

$$\phi(x)=\phi_S+F(x-b), \qquad F=(1/b)(\phi_S-\phi_M-eV). \quad \text{(C2c)}$$

The applied bias V is positive when the p-type semiconductor is positive relative to the metal electrode. For a metal-insulator-semiconductor junction, the $\mathbf{k}_{\parallel}$ integration is over the region

$$0\leq\hbar^2k_{\parallel}^2/2m^*\leq(\xi_k+\zeta), \quad \text{(C3)}$$

where m^* is the effective mass of the light (heavy) holes. The Fermi level falls a distance ζ below the valence-band edge, and the light (heavy) hole band energy is given by

$$E(\mathbf{k})=-\hbar^2k^2/2m^*=-(\xi_k+\zeta). \quad \text{(C4)}$$

The variable ϵ is the total energy measured relative to the Fermi level in the semiconductor, so that (in a one-electron calculation for holes)

$$\epsilon=-\xi_k. \quad \text{(C5)}$$

The velocity of the holes is denoted by v_{Rx}, whereas the velocity of the metal electrons is given by v_{Lx} which is taken to be the metal Fermi velocity $\hbar k_{FL}/m_L$. Conservation of $\mathbf{k}_{\parallel}$ was assumed as is appropriate for elastic specular tunneling through an average potential barrier (see Sec. 7 of Ref. 3).

Three important consequences of the calculation should be discussed.

(a) For changes of the barrier thickness from 10 to 15 Å, it was found that the conductance varied by a factor $\sim10^3$, but the shape or the normalized conductance was found to be virtually independent of the barrier thickness. Hence, only the shape or the normalized conductance was significant in determining the appropriate value of the Fermi degeneracy ζ. The magnitude of the conductance should be fit easily with the proper choice of the barrier thickness $b=11$ Å.

(b) We can determine the Fermi degeneracy ζ unambiguously by fitting the slope of the normalized conductance curve in the linear region ($V<60$ mV). In the example shown in Fig. 9, if we had taken $\zeta>120$ meV, the calculated curve would have been flatter, or if we had taken $\zeta<120$ meV, the calculated curve would have been steeper than the experimentally measured curve. The resulting value of the effective number of free holes is $n=7.9\times10^{19}$ cm^{-3}, neglecting nonparabolicity of the bands.

(c) The calculated conductance was found to be slightly negative for biases greater than ~108 mV. Including the field penetration into the semiconductor in this calculation gave values of the conductance in this region which were positive. It should be noted that even the rather large value of $\phi_S-\phi_M=0.75$ eV used in our calculation did not give positive values of dI/dV in this region of the magnitude observed experimentally, unless the doping was assumed to be somewhat less ($\sim5\times10^{19}$ cm^3), however. This result is probably due to the occurrence of incoherent fluctuation-potential channels for current flow in air-cleaved junctions (see Sec. 7 of Ref. 3).

We should state that the numerical calculations provide only a convenient parametrization of the experimentally measured conductance, and do not provide an independent check of the one-electron tunneling theory as did the measurements on n-Ge.[25]

Let us now derive a simple expression for the barrier-penetration factor D based upon the results of Appendix B. (a) The invariance of the conductance line shapes to small changes in the barrier parameters indicates that the height of the barrier (~4 eV) is large enough so that changes in ξ_k, eV, and $\hbar^2k_{\parallel}^2/2m^*$ ($\lesssim100$ mV) can be treated by expanding the WKB exponent.[50] From Sec. 2, we recall that the phase-space integration

$$\int\frac{d^2k_{\parallel}}{(2\pi)^2}D(\mathbf{k}_{\parallel},\xi_q)$$

determines the general shape of the conductance curve. In fact, since the barrier-penetration factor is slowly varying in the region of interest

$$\int\frac{d^2\mathbf{k}_{\parallel}}{(2\pi)^2}D(\mathbf{k}_{\parallel},\xi_k)\simeq\frac{D(0,\xi_k)}{(2\pi)^2}\pi\frac{2m^*}{\hbar^2}(\xi_k+\zeta). \quad \text{(C6)}$$

We note that $\pi(2m^*/\hbar^2)(\xi_k+\zeta)$ is the available area in phase space and that such a form is readily derived from

[49] K. H. Gundlach, Solid State Electron. 9, 949 (1966).

[50] E. L. Murphy and R. H. Good, Jr., Phys. Rev. **102**, 1464 (1956); R. Stratton, *ibid.* **135**, A794 (1964).

the WKB approximation.[13] The prefactors of the WKB exponential are slowly varying except near the band edge. The important value of ξ_k in determining the conductance is

$$\xi_k = -eV. \tag{C7}$$

Substituting Eq. (C7) into (C6), we find that in this approximation

$$dI/dV \propto (-eV+\zeta). \tag{C8}$$

This prediction describes the observed behavior of the experimental dI/dV in the region ($V \leq 60$ mV), although, in the analysis of the line shapes, we used a more accurate approximation than Eq. (C6). Equations (C7) and (C8) illustrate the important fact that for the injection or extraction of carriers near the band edge in an electrode in which only one band contributes to the current, the conductance is determined primarily by the avaiable area in phase space.

If we now take into account the dependence of D upon ξ_k, eV, and $\hbar^2 k_{11}^2/2m^*$ to first order in the exponent, we can write

$$D = D_0 \exp\left(\frac{eV}{E_1} - \frac{(\xi_k+eV)}{E_0} - \frac{\hbar^2 k_{11}^2}{2m_b E_0}\right) \tag{C9a}$$

$$= D_0 \exp\left(\frac{eV}{E_1} + \frac{\xi_q}{E_0} - \frac{\hbar^2 k_{11}^2}{2m_b E_0}\right), \tag{C9b}$$

where D_0 is a constant and

$$E_0 = \left(\frac{\hbar^2}{2m_b}\right)^{1/2} \frac{\phi_S - \phi_M}{2b(\phi_S^{1/2} - \phi_M^{1/2})}, \tag{C9c}$$

$$E_1 = \left(\frac{\hbar^2}{2m_b}\right)^{1/2} \frac{\phi_S - \phi_M}{2b}\left[\phi_S^{1/2} - \frac{2}{3}\frac{\phi_S^{3/2} - \phi_M^{3/2}}{\phi_S - \phi_M}\right]^{-1}, \tag{C9d}$$

$$\xi_q = -\xi_q - eV. \tag{C9e}$$

For the barrier shown in Fig. 10, $\frac{1}{2}E_1 \cong E_0 \cong 500$ meV. In general, we have regarded E_0 and E_1 as adjustable parameters to be determined from the experimental data. To limit the number of parameters, however, we always take $E_1 = 2E_0$.

Neglecting the bias dependence of D, it can be shown that for the barrier-penetration factor (C9), the conductance is given by

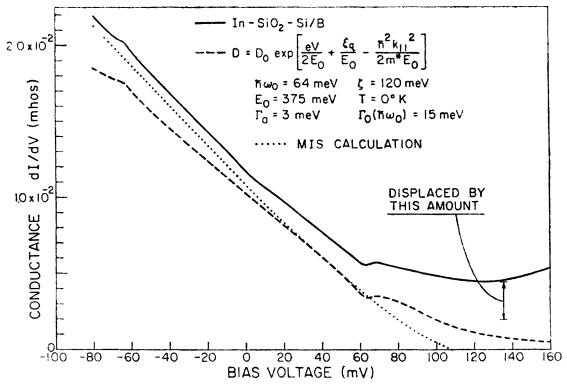

FIG. 11. Comparison of the conductance resulting from the model barrier-penetration factor (dashed curve), as given by Eq. (C9b) with $E_1 = 2E_0$ and the self-energy given by Eqs. (A2.2)–(A2.6), to the numerical calculation of metal-insulator-semiconductor conductance (dotted curve) of Fig. 10 and to the experimental data (solid curve) for p-Si (Ref. 24).

$$\frac{dI}{dV} = \frac{4\pi e^2 m_b E_0 A}{\hbar^3} D_0 e^{eV/E_1} \times\left[1 - \exp\left(-\frac{m^*}{m_b}\frac{(-eV+\zeta)}{E_0}\right)\right]. \tag{C10}$$

In Fig. 11, we show a comparison of the model conductance (C10) with experimental data and with the numerical calculation shown in Fig. 10. For simplicity we have taken $m^* = m_b$ (which holds quite well for the heavy holes), and $\frac{1}{2}E_1 = E_0 = 375$ meV. Also shown is the effect of strong hole phonon coupling near $eV = \pm\hbar\omega_0$, the phonon energy, which is discussed in text of this paper.

To obtain a more accurate expression for the one-electron conductance, we can account for the contribution due to the voltage dependence of D by adding, to the right-hand side of Eq. (C10), the correction term

$$\left(\frac{dI}{dV}\right)_c = \frac{-4\pi e^2 m_b E_0^2 A}{\hbar^3 E_2} \exp\left(-\frac{eV}{E_2}\right)\left\{\exp\left(\frac{eV}{E_0}\right) - 1 - \tfrac{1}{2}e^{-\zeta/E_0}\left[\exp\left(\frac{2eV}{E_0}\right) - 1\right]\right\}, \tag{C11a}$$

where

$$E_2^{-1} = E_0^{-1} - E_1^{-1}. \tag{C11b}$$